

# GaussianVideo: Efficient Video Representation via Hierarchical Gaussian Splatting

Andrew Bond<sup>1,\*</sup> Jui-Hsien Wang<sup>2</sup> Long Mai<sup>2</sup> Erkut Erdem<sup>3</sup> Aykut Erdem<sup>1</sup>  
<sup>1</sup>Koç University <sup>2</sup>Adobe Research <sup>3</sup>Hacettepe University

<https://cyberiaada.github.io/GaussianVideo/>

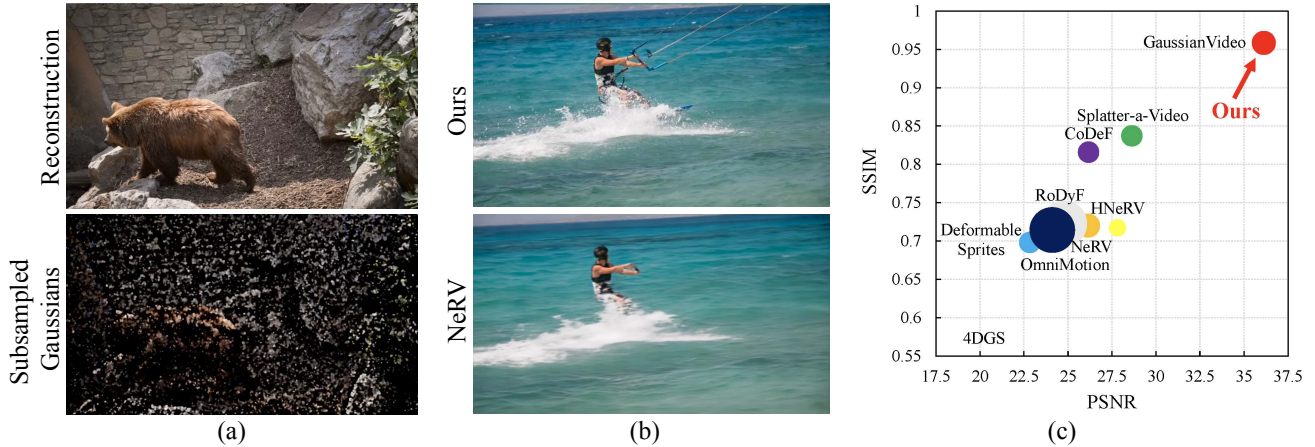


Figure 1. **We present GaussianVideo – a new Gaussian Splatting framework for representing videos** that effectively models in-the-wild videos, while maintaining training efficiency and capturing semantic motions with minimal supervision. (a) We can render the  $960 \times 540$  video at 93 FPS on an NVIDIA A40 GPU. (b) Our reconstruction PSNR on this video achieves 44.21 compared to NeRV [2] at 29.36, representing a 50.6% improvement. (c) On the DAVIS [6] dataset, our approach balances reconstruction quality with training time (dot size in log scale).

## Abstract

Efficient neural representations for dynamic video scenes are critical for applications ranging from video compression to interactive simulations. Yet, existing methods often face challenges related to high memory usage, lengthy training times, and temporal consistency. To address these issues, we introduce a novel neural video representation that combines 3D Gaussian splatting with continuous camera motion modeling. By leveraging Neural ODEs, our approach learns smooth camera trajectories while maintaining an explicit 3D scene representation through Gaussians. Additionally, we introduce a spatiotemporal hierarchical learning strategy, progressively refining spatial and temporal features to enhance reconstruction quality and accelerate convergence. This memory-efficient approach achieves high-quality rendering at impressive speeds. Experimental results show that our hierarchical learning, combined with robust camera motion modeling, captures complex dynamic scenes with strong temporal consistency, achieving state-of-

the-art performance across diverse video datasets in both high- and low-motion scenarios.

## 1. Introduction

Videos are traditionally represented as a sequence of frames, each of which is a 2D grid of discrete pixels with fixed resolutions. Recently, it has become feasible to model the continuous nature of videos using implicit representations such as NeRFs [2], by modeling the videos as neural networks that output whole frames. It was shown that this is a promising direction in replacing the decade-old frame-based representation, and encoding and decoding speed can both be improved along with reconstruction quality.

On the other hand, 3D Gaussian Splatting (3DGS) [10] has been gaining popularity in modeling 3D scenes as an alternative implicit representation. Compared to NeRFs, 3DGS-based methods enable faster rendering speed and smaller memory usage, and their continuous and interpretable representations allow applications such as stylization [11], 3D editing [5], frame interpolation [27], novel-

\* Done during an internship at Adobe Research.

view synthesis [10], and inverse rendering [14]. Recently, GaussianImage [37] showed that Gaussian splatting can also be applied to represent images. Leveraging the fixed-viewpoint nature of images, and optimization techniques and codecs designed specifically for Gaussians, they showed that replacing pixels with Gaussians can be feasible and more efficient for rendering images. Furthermore, Splatter-a-Video [27] explored modeling videos using Gaussians. They showed that by utilizing a myriad of supervisory signals such as optical flow, depth, segmentation maps, and others at training, the obtained GS-based representation can be very versatile for downstream processing while maintaining good reconstruction quality.

In this paper, we introduce a lightweight framework for modeling videos using Gaussians. Similar to Splatter-a-Video, our design goals are twofold: (1) to achieve high-quality and efficient video reconstruction, and (2) to support downstream applications such as frame interpolation, spatial resampling, editing, and more. We posit that enabling these applications requires the dynamics of the Gaussians to be highly semantic and coherent. Unlike Splatter-a-Video, we seek an approach that results in this type of semantic movement of the Gaussians as an *emerging* behavior, rather than being forced by the auxiliary supervisory signals (see Fig. 2 for illustration). This is because these supervisory signals can themselves be expensive to compute and challenging to be accurately extracted; in addition, they might hide the negative effects of the design choices made in the representation itself. For this purpose, we propose several novel techniques to model the videos and regularize the movements of Gaussians. The main technical contributions of the paper are as follows:

- We introduce a B-spline-based motion representation that models smooth motion trajectories of scene elements, ensuring temporal consistency while allowing for local variations in motion (§3.2)
- We propose a novel hierarchical learning strategy that refines spatial and temporal features of the Gaussian representation, leading to improved reconstruction quality and faster convergence compared to existing methods (§3.3)
- We develop an approach to learning continuous camera motion using Neural ODEs, removing the dependency on precomputed camera parameters and enhancing adaptability to different capture setups (§3.4).
- Our method significantly reduces memory usage and training time, achieving state-of-the-art performance on standard video datasets with lower computational resources compared to previous approaches.

An overview of our approach is illustrated in Fig. 3. Our method surpasses existing approaches in reconstruction quality and temporal consistency, effectively handles videos with varying levels of camera and object motion, and achieves competitive training times and memory efficiency.

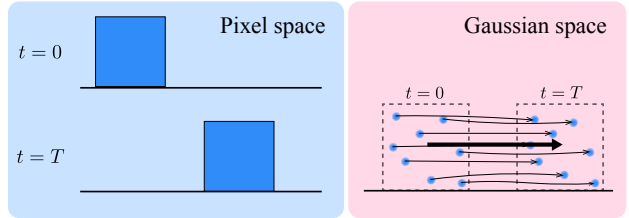


Figure 2. **A toy example illustrating the semantic and coherent motion of the underlying Gaussians.** Rather than relying on strong supervisory signals like optical flow during training, we carefully design a Gaussian parametrization tailored for video modeling to naturally encourage this behavior, and demonstrate its effectiveness in downstream applications.

## 2. Related Work

### 2.1. Implicit Neural Video Representations

Recent work have shown that neural networks can be used to represent various types of multimedia signals [24], including images [25], videos [2], and audio [26]. For videos, in contrast to traditional frame-based video representations, these neural video representations provide more compact and flexible modeling. NeRV [2] was the first implicit representation that models an entire video using MLPs by mapping timesteps to frames. HNeRV [3] extends this approach by employing a hybrid representation with content-adaptive embeddings, alongside a balanced parameter distribution across the network, enhancing efficiency and adaptability. DS-NeRV [34] decomposes videos into static and dynamic codes, which are co-optimized during training to capture both persistent and transient video elements. Meanwhile, Splatter-a-Video [27] uses Gaussian splatting to represent videos, but with supervision such as segmentation masks, depth maps, optical flow, and feature maps.

### 2.2. Dynamic Gaussian Splatting

3D Gaussian Splatting (3DGS) [10] was originally introduced as a method to learn static 3D scenes. However, significant efforts have since extended this approach to dynamic scenes. Spacetime GS [13] models the positions and rotations with polynomials, represents colors through an MLP, and employs radial basis functions for opacities. 4DGS [32] advances this framework by utilizing a learned deformation network parametrized by an MLP to predict the offsets of position, rotation, and scales over time. Meanwhile, DynMF [12] uses a learned motion basis of distinct motions in a scene, with each motion trajectory parameterized by a small MLP. MotionGS [38] employs optical flow to decouple camera motion from object motion, allowing for more constrained deformation of Gaussians. Recently, constrained approaches to dynamic Gaussian splatting, such as [28], have emerged to efficiently learn volumetric videos

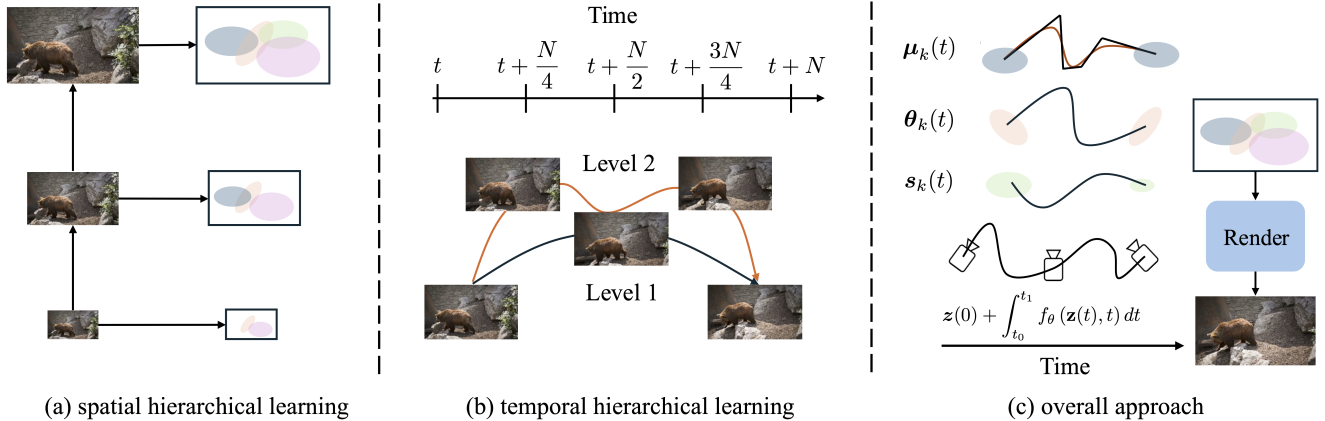


Figure 3. **Overview of the GaussianVideo approach for neural video representation.** Our method combines 3D Gaussian splatting with continuous camera motion modeling via Neural ODEs to handle dynamic scenes efficiently. The pipeline includes hierarchical learning strategies for both (a) spatial and (b) temporal domains, progressively refining Gaussians to capture fine details and smooth motion.

with a reduced Gaussian count. In this paper, we focus on adapting the 3DGS formulation to model video data instead of modeling dynamic 3D scenes.

### 2.3. Camera Modeling

The standard approach for obtaining camera information from images is COLMAP [23], a type of Structure-from-Motion (SfM) algorithm. However, recently there have been attempts to replace COLMAP with a deep-learning based approach. Dust3r [30] uses an unconstrained image collection to predict a point cloud as well as intrinsic and extrinsic camera information, but crucially requires at least two images. Alternatively, some works, such as [7], try to avoid the use of COLMAP by progressive training which predicts Gaussian transformations between steps.

## 3. Method

### 3.1. Background

**Gaussian Splatting.** Gaussian Splatting reconstructs a scene in  $d$  dimension by optimizing a set of Gaussians [10], each of which is parameterized by position  $\mu \in \mathbb{R}^d$ , covariance  $\Sigma \in \mathbb{R}^{d \times d}$ , colors with spherical harmonics  $\mathbf{c} \in \mathbb{R}^{(d_c+1)^2}$ , and opacity  $o \in \mathbb{R}$ .  $d_c$  is the order of spherical harmonics. In the forward pass, the Gaussians are projected and rasterized onto the observed image planes, and through standard reconstruction loss the parameters can be optimized. The covariance matrix can be further parametrized using a decomposition  $\Sigma = (\mathbf{RS})(\mathbf{RS})^T$ , where  $\mathbf{R}$  is a rotation matrix and  $\mathbf{S}$  is a (diagonal) scaling matrix.

**Neural ODEs.** A Neural ODE [4] is a continuous-depth model in which the continuous dynamics of the hidden units are parametrized using a differential equation, where the function being differentiated is a neural network. Specif-

ically, given some initial condition  $\mathbf{z}(0)$ , the Neural ODE solves the following equation

$$\mathbf{z}_{dT} = \mathbf{z}(0) + \int_{t_0}^{t_1} f_{\theta}(\mathbf{z}(t), t) dt, \quad (1)$$

where  $f_{\theta}$  is the network parametrization. The initial condition can be learned, or predicted using another network.

### 3.2. Adding Dynamics to the Gaussians

Videos contain a lot of redundant information. For example, frames in a video of someone walking down the street will share many similarities, such as the color of the shirt or the shades in the sky. To model this temporal aspect, we augment the parameters of the Gaussians with temporal basis functions. Below, we discuss various choices and explain our design choices.

We found that the conventional polynomial basis such as those used in [13, 15, 27] to model positional changes can cause overfitting and reconstruction errors for even simple trajectories such as a U-shape (see Fig. 4). Unsurprisingly, this is because a single polynomial at low order does not approximate complex trajectories well, especially those from a video of long duration or high dynamics; at high order, polynomials are known to be unstable and sensitive to noise. Fortunately, this problem is well studied in computer graphics and approximation theory [19]. We show that a simple adoption of basic cubic B-splines can greatly alleviate this issue (see Fig. 4). Specifically, we model the positions of the  $n$ -th Gaussians as a time-dependent function

$$\mu_n(t) = \sum_{i=0}^N N_{i,p}(t) \mathbf{P}_{n,i}, \quad (2)$$

where  $\mathbf{P}_{n,i} \in \mathbb{R}^d$  is the  $i$ -th control point, and  $N_{i,p}$  are the  $p$ -th degree basis functions. We use  $p = 3$  for a common

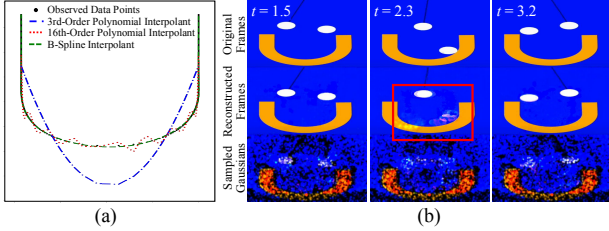


Figure 4. **Polynomial basis functions, widely used for temporal modeling, can introduce reconstruction errors and instability,** as shown in this example. (a) 3rd-order polynomial fails to fit the U-shape trajectory, while the commonly used 16th-order polynomial fits better, but is unstable and sensitive to small perturbations (see the bottom part of the “U”). In contrast, our cubic B-spline formulation (green dashed lines) fits the shape is unstable and sensitive to small perturbations due to its flexibility. (b) When using a low-order polynomial for motion fitting, the white ball following the “U” disappears entirely in the middle frame and reappears later, highlighting the instability of single-polynomial modeling.

cubic spline.  $N$  is the number of control points. We use clamped B-splines and thus the first  $p + 1$  knots are fixed at 0, and the last  $p + 1$  knots are fixed at 1; the rest of the knots are evenly spaced.

In contrast, for other degrees of freedom, such as covariance (through rotation and scaling matrices), color, and opacity, we intentionally use less expressive models. This is because (1) if opacity and scaling are allowed to change dramatically, the reconstruction loss tends to push the Gaussians to become insignificant. For example, if the opacity of a Gaussian is allowed to vary over time, we found that on average 80 – 85% of the Gaussians will have low opacity ( $o < 0.5$ ). Similarly, if scaling is allowed to change dramatically, Gaussians tend to shrink in size and become insignificant. Both cause inefficient utilization of the available degrees of freedom and will negatively impact convergence and training time. We therefore do not allow opacity to change over time, resulting in much fewer Gaussians having low opacity ( $< 5\%$ ); for covariances, we use a regular 3rd-order polynomial to model the scaling and rotation, similar to Li et al. [13]. (2) A popular choice for modeling the color of the Gaussians is through a learned MLP [13]; however, we found that even a weak MLP encourages the Gaussians to change colors rather than move around to follow entities in the video. We therefore do not allow the color to change over time either. More analysis of these design choices is provided in the supplemental material.

In summary, the dynamics of the  $n$ -th Gaussian is parametrized by

$$\tilde{\mathcal{G}}_n(t) = \mathcal{G}_n \left( \underbrace{\mu_n(t)}_{\text{B-splines}}, \underbrace{\Sigma_n(t)}_{\text{3rd-order polynomials}}, \underbrace{\mathbf{c}_n}_{\text{constant}}, \underbrace{o_n}_{\text{constant}} \right) \quad (3)$$

to properly capture the motions in the videos yet maintain modeling efficiency and semantics of the representation.

### 3.3. Hierarchical Representations of the Gaussians

Inspired by the Multigrid methods [8] in solving differential equations and other hierarchical representations in the Gaussian Splatting literature [9, 18], we also propose to decompose the optimization into discrete stages, each targeting different levels of details. By building the representation progressively at several different spatial and temporal scales, from coarse to fine, we found that it results in more efficient learning performance.

**Spatial Hierarchical Learning.** We first introduce our spatial hierarchical learning approach using the Gaussian pyramid. Recall that a Gaussian pyramid contains several levels of the same image, each with a progressively downsampled version of itself using Gaussian kernel [1]. This naturally fit into a Gaussian splatting framework because, intuitively, a point at a lower level of the pyramid can be represented by a single Gaussian perfectly at a higher level due to the kernel choice. And when the higher levels get reprojected back to lower levels (higher resolutions), the only thing that needs changing to continue to fit is the single scalar scale of this Gaussian. Using this rationale, our spatial hierarchy starts the training with the highest level of the pyramid (or coarsest spatial details), trains it to convergence. We then move down one level, introduce more Gaussians, and again train it to convergence. We repeat this process until all  $N_p$  levels in the pyramid are trained.

**Temporal Hierarchical Learning.** To promote smooth motion that is useful for downstream applications such as frame interpolation (§5), we similarly adopt a progressive frame sampling approach based on B-splines. We start by training on every  $N$ -th frame, then progressively increase the temporal resolution, optionally refining the B-spline knots to introduce additional flexibility without disrupting the learned Gaussian movements.

**Spatio-Temporal Hierarchical Learning.** By combining these spatial and temporal hierarchies, we can construct a Gaussian video model that captures both global structure and local details, while also exhibiting smooth, natural motion over time. We validate these claims in §4.

### 3.4. Modeling Camera Motion

Our approach described so far performs well on videos without camera motion but is sensitive to even slight camera shifts. Existing approaches typically rely on Structure-from-Motion (SfM) algorithms such as COLMAP [23] to estimate camera parameters [10, 27]. However, this can be unreliable for single-camera videos, as the limited perspectives make it difficult to accurately reconstruct the camera motion. Furthermore, COLMAP is a slow process, making



it a bottleneck for training efficiency.

To address these issues, we propose a simple yet effective approach to learning camera parameters directly within our video reconstruction pipeline. Since the forward pass of our framework already encompasses the entire rendering process, the key insight is that both intrinsic and extrinsic camera parameters can be explicitly learned and subsequently used to render the Gaussians. Specifically, we model the intrinsic parameters (i.e., focal length and principal points) with constants held throughout the video; for extrinsic parameters (i.e., rotation and translation of the camera), we model them with neural ODEs. Details for the camera modeling are given in the supplementary material.

Further optimization can be done to disable camera modeling for videos without significant camera motion, such as those of the DAVIS dataset (see Table 1), to learn more efficiently. However, for simplicity, all our experiments always utilize the full camera modeling pipeline. We implemented the camera modeling as custom CUDA kernels for efficient forward and backward passes; this tight integration between camera parameters and rendering pipeline allows for optimized training performance by minimizing memory transfer between devices.

## 4. Results

### 4.1. Experimental Setup

**Datasets.** We validate our approach experimentally on two datasets: DL3DV [16] and DAVIS Tap-Vid benchmark [6]. The DL3DV dataset enables testing our approach on high-camera-motion scenes, while the DAVIS dataset allows us to assess performance on lower-motion scenes with a focus on fine detail. Furthermore, the DAVIS dataset allows for a comparison with Splatter-A-Video [27]. In particular, we use the 1K split of the DL3DV dataset at 540p resolution, in which the videos are 30 or 60 FPS, and the videos last for between 5-10 seconds on average. Furthermore, while the DL3DV dataset does come with provided camera information, we do not use them in order to ensure our model is able to learn the camera dynamics by itself. To fairly compare against Splatter-a-Video, we use the DAVIS dataset at 480p resolution, with videos lasting for a few seconds at 30 FPS.

**Evaluation Metrics.** Following existing work, we employ the peak signal-to-noise ratio (PSNR), structural similarity index (SSIM) [31] metrics, and learned perceptual image patch similarity (LPIPS) [36] perceptual image quality metric to assess the video reconstruction performance of the approaches.

**Implementation Details.** We conduct all experiments on both datasets with a consistent set of hyperparameters and experimental setup. Specifically, we use 400K Gaussians, trained for 50K timesteps, with a learning rate of 0.01 that decays exponentially with a factor of  $\gamma = 0.99995$ . Follow-

ing [37], we employ the Adan [33] optimizer. Gaussians are initialized randomly within a radius of three times the camera width/height, ensuring Gaussians are present regardless of the learned camera motion trajectory.

The results reported here are based on the standard L2 reconstruction loss. Although additional regularization objectives can be used for specific downstream tasks, our primary focus is on optimizing reconstruction quality.

We apply the spatial and temporal hierarchical learning procedure once, after 15K training steps. At this point, adding 100K new Gaussians to capture fine details from upsampling. Additionally, every 5K steps, we identify all Gaussians that do not appear on any frames of the video, and *warp* them to the first frame by adjusting the splines of their means. During this warping, we identify the regions of high error and move them to these regions. This procedure is stopped after 30K steps, as camera motion changes minimally beyond this point.

Finally, while it is common when using spherical harmonics to use a progressive learning scheme that first learns the 0th-order coefficients and gradually increases the order over time, we found that this performs worse than learning all the coefficients at once. This is due to the camera position changing frequently during the early stages of training, which causes a lot of noise with the spherical harmonics.

### 4.2. Experimental Results

Table 1 compares our results with several existing methods across both datasets. Our approach consistently achieves the best scores on all three evaluation metrics for both datasets. Fig. 5 provides qualitative comparisons of reconstruction quality for the evaluated methods on three sample sequences from the DL3DV dataset. In these examples, we observe that other approaches struggle with high-frequency details, such as edges. For instance, in the store scene, other methods fail to accurately reconstruct the edges of the shelf, while our approach preserves fine details along the edge. GaussianImage, which is trained on a frame-by-frame reconstruction task, achieves good reconstruction results due to parameter scaling with the number of frames. However, this approach lacks temporal consistency across frames, as no relationship is established between Gaussians in different frames, making it difficult to maintain consistency in downstream applications.

### 4.3. Analysis

**Ablation Study.** To validate each component we introduced, we conducted an extensive ablation study across various components, summarized in Table 2. We evaluate different configurations in our pipeline, including using a static camera instead of employing a Neural ODE, omitting camera representation entirely (as in GaussianImage), replacing splines with polynomials, applying progressive SH coeffi-

Model	PSNR $\uparrow$	SSIM $\uparrow$	LPIPS $\downarrow$	Training Time
<b>DL3DV Dataset</b>				
GaussianVideo (Ours)	43.21	0.99	0.013	~ 45 mins
GaussianImage [37]	38.68	0.95	0.097	~ 15 mins
NeRV [2]	28.50	0.87	0.184	~ 45 mins
HNeRV [3]	30.32	0.86	0.183	~ 15 mins
3DGS [10]	29.82	0.92	0.120	2.1 hr
<b>DAVIS Dataset</b>				
GaussianVideo (Ours)	37.38	0.96	0.021	~ 45 mins
GaussianImage [37]	36.25	0.94	0.045	~ 15 mins
Splatter-a-Video [27]	28.63	0.84	0.228	~ 30 mins
NeRV [2]	26.15	0.72	0.312	~ 45 mins
HNeRV [3]	27.82	0.72	0.252	~ 15 mins
4DGS [32]	18.12	0.57	0.394	~ 40 mins
RoDyF [17]	24.79	0.72	0.394	> 24 hrs
Deformable Sprites [35]	22.83	0.70	0.301	~ 30 mins
OmniMotion [29]	24.11	0.72	0.371	> 24 hrs
CoDeF [20]	26.17	0.82	0.290	~ 30 mins

Table 1. **Comparison of our approach with various methods on the DL3DV [16] and DAVIS [6] datasets.** Our method achieves the best performance across all metrics among video representation learning models. Most results for the DAVIS dataset are obtained from the Splatter-A-Video work, which doesn’t provide parameter counts. The **best**, the **second best**, and the **third best** results are highlighted.

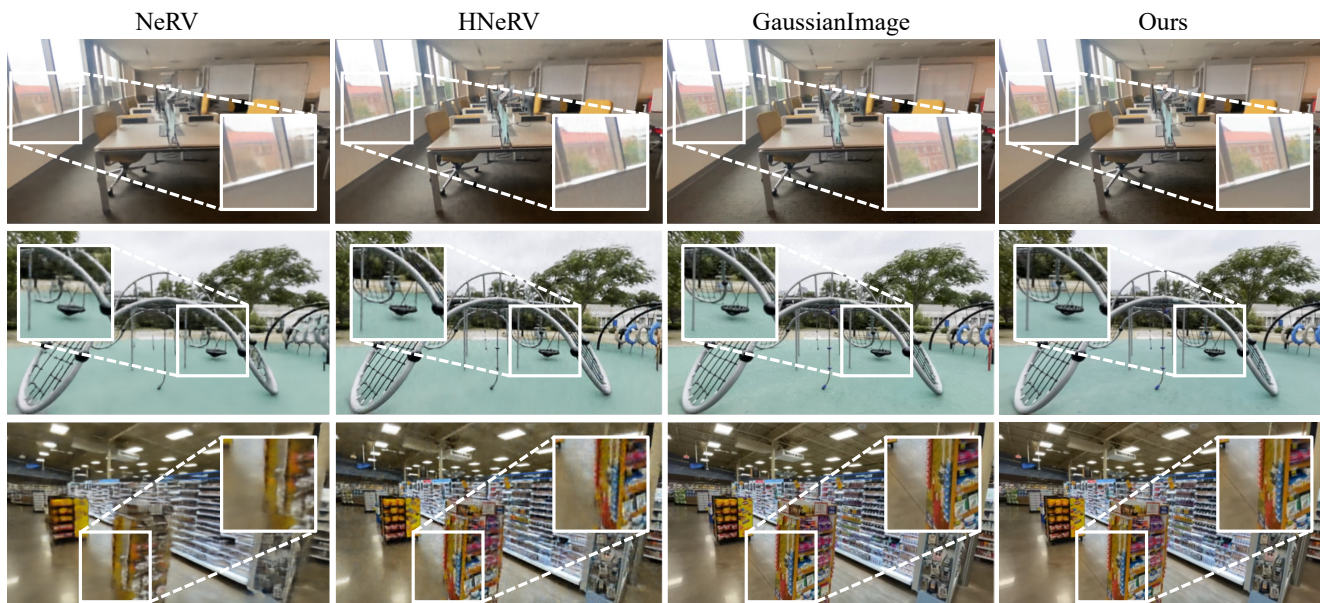


Figure 5. **Video reconstruction results on the DL3DV dataset**, comparing GaussianVideo with alternative video representation models including NeRV, HNeRV, and GaussianImage. Each sequence shows reconstructed frames, highlighting GaussianVideo’s ability to capture fine spatial details and structural fidelity, even in high-motion scenes.

cient learning, using fixed scales over time, and avoiding the warping unrendered Gaussians. Our findings show that any form of learned camera representation is advantageous, with a substantial performance gain achieved by modeling

camera motion using a Neural ODE. Additionally, we assess the impact of hierarchical learning, testing spatial-only, temporal-only, and combined hierarchical learning, as well as a setup without hierarchical learning. Both spatial and

Setting	PSNR $\uparrow$	SSIM $\uparrow$	LPIPS $\downarrow$	Training Time
GaussianVideo Full Model (Baseline)	43.2110	0.9882	0.0125	$\sim$ 45 mins
Temporal Hierarchical Learning Only	42.8404	0.9871	0.0142	$\sim$ 45 mins
Spatial Hierarchical Learning Only	42.2068	0.9846	0.0224	$\sim$ 35 mins
No Hierarchical Learning	40.2016	0.9820	0.0177	$\sim$ 40 mins
Static Camera (Fixed Learned Position)	33.9304	0.9238	0.1011	$\sim$ 35 mins
No Camera Model	21.1821	0.7600	0.3042	$\sim$ 20 mins
Polynomial Motion Representation	20.1871	0.6107	0.3991	$\sim$ 30 mins
Incremental Spherical Harmonics Coefficients	31.0736	0.8594	0.1644	$\sim$ 40 mins
Fixed Gaussian Scale Over Time	34.1585	0.9304	0.0951	$\sim$ 40 mins
Static Unused Gaussians (No Warping)	34.0106	0.9247	0.1002	$\sim$ 35 mins

Table 2. **Performance evaluation of various configurations in our ablation study on the DL3DV dataset.** We compare key components of the GaussianVideo pipeline such as camera representation, motion modeling, and hierarchical learning strategies.

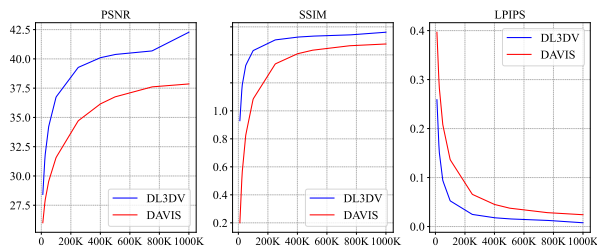


Figure 6. **Effect of Gaussian count on performance metrics.**

temporal hierarchical learning yield notable improvements individually, yet their combination consistently produces the best results. Notably, the spatial hierarchical learning procedure also reduces training time, as the initial phase of training involves fewer, lower-resolution Gaussians.

**Effect of Gaussian Count on Model Performance.** To understand the influence of the number of Gaussians on performance, we test our approach on both datasets with Gaussian counts ranging from 1,000 to 1 million, training each configuration for 50K steps. As shown in Fig. 6, even with only 100K Gaussians, our method achieves superior performance on both datasets compared to existing video-based approaches. However, performance plateaus around 400K Gaussians, beyond which further increases in Gaussian count provide minimal improvement while significantly extending training time.

**Impact of Training Steps on Performance Metrics.** We also investigate the effect of training duration on performance, testing a range of training lengths from 5K to 100K steps, with all experiments utilizing 400K Gaussians. As seen in Fig. 7, even with 30K timesteps, our approach outperforms the prior video-based methods. Based on these findings, we select 50K timesteps as it offers a balance between high metric performance and training efficiency.

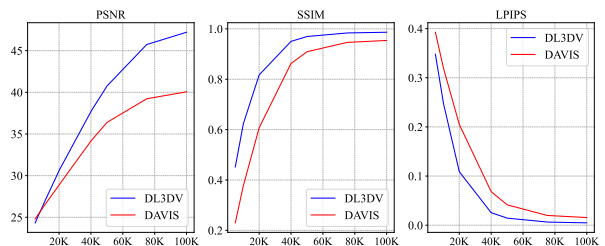


Figure 7. **Impact of training duration on performance metrics.**

## 5. Applications

One of the advantage of our Gaussian video representation is the learned continuous nature. Although downstream applications are not the focus of the paper, we designed our method to ensure the learned Gaussian dynamics are semantic and coherent (see Fig. 2). To illustrate its potential, below we demonstrate a few applications.

**Frame Interpolation.** Leveraging continuous motion representation for the Gaussians allows us to interpolate frames at arbitrary timesteps, including those not seen during training. Fig. 8 illustrates this process, showing the input left and right frames along with four intermediate interpolated frames. These interpolated frames successfully capture the realistic non-rigid motion of the cow’s legs, demonstrating the model’s ability to maintain natural motion dynamics across unseen timesteps.

**Spatial Resampling.** The inherently spatial nature of our Gaussian video representation allows for making arbitrary adjustments in the spatial resolution of the learned videos. This is achieved by modifying the scale parameters along with the principal point and focal lengths of the learned camera parameters, using simple scaling operations. In Fig. 9, we demonstrate such a spatial resampling procedure where the frame width is divided by  $1.5\times$  and the height is multiplied by  $1.5\times$ . The GaussianVideo representation



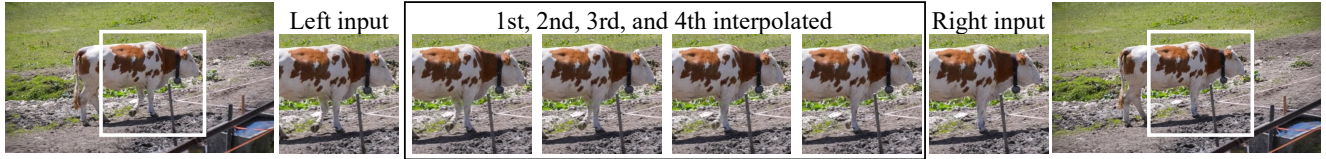


Figure 8. **Frame interpolation results for GaussianVideo using continuous motion representation.** The close-up views show the input left and right frames, along with intermediate interpolated frames, successfully capturing the realistic non-rigid motion of the cow’s legs.



Figure 9. **Spatial resampling results on a learned video.** In this example, the frame height is scaled by  $1.5\times$ , and the width is reduced by  $1.5\times$ , demonstrating the model’s ability to adjust resolution while preserving sharpness and detail. This is achieved by modifying scale parameters, as well as the principal point and focal lengths of the learned camera parameters, allowing for viewport adjustments beyond traditional resampling methods.

effectively maintains high-quality reconstruction, free from artifacts, despite the significant spatial adjustments.

**Video Stylization.** For video stylization, we adopt the approach from [27]. Specifically, we use an existing image editing model to edit the first frame, then propagate these changes across the entire video with a reconstruction loss, updating only the spherical harmonics coefficients. While there exist some works that perform stylization using Gaussian splatting, we focus on a straightforward approach that does not require extensive extra supervision, such as CLIP [22] losses. Fig. 10 shows an example where a fire image is first used to edit the initial frame, which is then propagated throughout the video in a consistent manner, such as the chair adopting a fire-like texture and the floor to the left of the table turning a vivid red.



Figure 10. **Video stylization results using GaussianVideo.** Starting with a ‘fire’ style applied to the first frame, the style is propagated across the video by updating only the SH coefficients, ensuring consistent stylization without additional supervision. The visual coherence across frames highlights GaussianVideo’s ability to maintain high-quality style transfer while preserving structural details throughout the sequence.

## 6. Conclusion

We introduced an efficient neural video representation method built on hierarchical Gaussian splatting, which tackles key challenges in dynamic scene representation, such as memory efficiency, reduced training times, and improved temporal consistency. By integrating B-spline-based motion trajectories with Neural ODE-driven camera modeling, our approach captures both static and dynamic elements without requiring prior camera parameters or heavy supervision. Our hierarchical learning strategy, operating across spatial and temporal domains, enables progressive refinement, yielding promising results in terms of evaluation metrics. Future work could explore the use of non-uniform rational B-spline (NURBS) [21] for greater motion flexibility and further optimize the spatial hierarchy to better utilize added Gaussians.

An important practical advantage of GaussianVideo is its capability to learn camera parameters directly as part of the optimization process, which is especially valuable in single-camera settings where traditional Structure-from-Motion techniques may fall short. With its efficient parameterization, competitive training times, and high-quality reconstruction, our approach is well-suited for applications such as dynamic scene representation and video editing. Further optimization for real-time rendering could broaden its applicability to scenarios requiring high fidelity and temporal stability.



## References

- [1] Peter J. Burt and Edward H. Adelson. The laplacian pyramid as a compact image code. *IEEE Transactions on Communications*, 31(4):532–540, 1983. 4
- [2] Hao Chen, Bo He, Hanyu Wang, Yixuan Ren, Ser-Nam Lim, and Abhinav Shrivastava. NeRV: Neural representations for videos. In *The Thirty-fifth Annual Conference on Neural Information Processing Systems (NeurIPS)*, 2021. 1, 2, 6
- [3] Hao Chen, Matt Gwilliam, Ser-Nam Lim, and Abhinav Shrivastava. HNeRV: A hybrid neural representation for videos. In *2023 IEEE Conference on Computer Vision and Pattern Recognition (CVPR)*, pages 23019–23019, 2023. 2, 6
- [4] Tian Qi Chen, Yulia Rubanova, Jesse Bettencourt, and David Kristjanson Duvenaud. Neural ordinary differential equations. In *The Thirty-second Annual Conference on Neural Information Processing Systems (NeurIPS)*, 2018. 3
- [5] Yiwen Chen, Zilong Chen, Chi Zhang, Feng Wang, Xiaofeng Yang, Yikai Wang, Zhongang Cai, Lei Yang, Huaping Liu, and Guosheng Lin. Gaussianeditor: Swift and controllable 3d editing with gaussian splatting. In *Proceedings of the IEEE/CVF Conference on Computer Vision and Pattern Recognition (CVPR)*, pages 21476–21485, 2024. 1
- [6] Carl Doersch, Ankush Gupta, Larisa Markeeva, Adria Recasens, Lucas Smaira, Yusuf Aytar, Joao Carreira, Andrew Zisserman, and Yi Yang. TAP-Vid: A benchmark for tracking any point in a video. In *The Thirty-sixth Annual Conference on Neural Information Processing Systems (NeurIPS)*, 2022. 1, 5, 6
- [7] Yang Fu, Sifei Liu, Amey Kulkarni, Jan Kautz, Alexei A. Efros, and Xiaocong Wang. Colmap-free 3d gaussian splatting. *2024 IEEE/CVF Conference on Computer Vision and Pattern Recognition (CVPR)*, pages 20796–20805, 2023. 3
- [8] Wolfgang Hackbusch. *Multi-Grid Methods and Applications*. Springer Berlin, Heidelberg, 1 edition, 1985. Topics: Numerical Analysis. 4
- [9] Abdullah Hamdi, Luke Melas-Kyriazi, Jinjie Mai, Guocheng Qian, Ruoshi Liu, Carl Vondrick, Bernard Ghanem, and Andrea Vedaldi. Ges : Generalized exponential splatting for efficient radiance field rendering. In *Proceedings of the IEEE/CVF Conference on Computer Vision and Pattern Recognition (CVPR)*, pages 19812–19822, 2024. 4
- [10] Bernhard Kerbl, Georgios Kopanas, Thomas Leimkuehler, and George Drettakis. 3D Gaussian splatting for real-time radiance field rendering. *ACM Transactions on Graphics (TOG)*, 42:1 – 14, 2023. 1, 2, 3, 4, 6
- [11] Áron Samuel Kovács, Pedro Hermosilla, and Renata G. Raidou. G-style: Stylized gaussian splatting. *Computer Graphics Forum*, page e15259, 2024. 1
- [12] Agelos Kratimenos, Jiahui Lei, and Kostas Daniilidis. DynMF: Neural motion factorization for real-time dynamic view synthesis with 3D Gaussian splatting. *ArXiv*, abs/2312.00112, 2023. 2
- [13] Zhan Li, Zhang Chen, Zhong Li, and Yinghao Xu. Spacetime Gaussian feature splatting for real-time dynamic view synthesis. In *2024 IEEE/CVF Conference on Computer Vision and Pattern Recognition (CVPR)*, pages 8508–8520, 2023. 2, 3, 4
- [14] Zhihao Liang, Qi Zhang, Ying Feng, Ying Shan, and Kui Jia. Gs-ir: 3d gaussian splatting for inverse rendering. In *Proceedings of the IEEE/CVF Conference on Computer Vision and Pattern Recognition (CVPR)*, pages 21644–21653, 2024. 2
- [15] Youtian Lin, ZuoZhuo Dai, Siyu Zhu, and Yao Yao. Gaussian-flow: 4d reconstruction with dynamic 3d gaussian particle. *arXiv:2312.03431*, 2023. 3
- [16] Lu Ling, Yichen Sheng, Zhi Tu, Wentian Zhao, Cheng Xin, Kun Wan, Lantao Yu, Qianyu Guo, Zixun Yu, Yawen Lu, et al. DL3DV-10K: A large-scale scene dataset for deep learning-based 3D vision. In *Proceedings of the IEEE/CVF Conference on Computer Vision and Pattern Recognition*, pages 22160–22169, 2024. 5, 6
- [17] Y. Liu, Chen Gao, Andreas Meuleman, Hung-Yu Tseng, Ayush Saraf, Changil Kim, Yung-Yu Chuang, Johannes Kopf, and Jia-Bin Huang. Robust dynamic radiance fields. *2023 IEEE/CVF Conference on Computer Vision and Pattern Recognition (CVPR)*, pages 13–23, 2023. 6
- [18] Tao Lu, Mulin Yu, Linning Xu, Yuanbo Xiangli, Limin Wang, Dahua Lin, and Bo Dai. Scaffold-gs: Structured 3d gaussians for view-adaptive rendering. In *Proceedings of the IEEE/CVF Conference on Computer Vision and Pattern Recognition*, pages 20654–20664, 2024. 4
- [19] Steve Marschner and Peter Shirley. *Fundamentals of Computer Graphics, Fourth Edition*. A. K. Peters, Ltd., USA, 4th edition, 2016. 3
- [20] Hao Ouyang, Qiuyu Wang, Yuxi Xiao, Qingyan Bai, Juntao Zhang, Kecheng Zheng, Xiaowei Zhou, Qifeng Chen, and Yujun Shen. Codef: Content deformation fields for temporally consistent video processing. *arXiv preprint arXiv:2308.07926*, 2023. 6
- [21] Les Piegl and Wayne Tiller. *The NURBS Book*. Springer-Verlag, New York, NY, USA, second edition edition, 1996. 8
- [22] Alec Radford, Jong Wook Kim, Chris Hallacy, Aditya Ramesh, Gabriel Goh, Sandhini Agarwal, Girish Sastry, Amanda Askell, Pamela Mishkin, Jack Clark, Gretchen Krueger, and Ilya Sutskever. Learning transferable visual models from natural language supervision. In *International Conference on Machine Learning*, 2021. 8
- [23] Johannes L. Schönberger and Jan-Michael Frahm. Structure-from-motion revisited. In *2016 IEEE Conference on Computer Vision and Pattern Recognition (CVPR)*, pages 4104–4113, 2016. 3, 4
- [24] Vincent Sitzmann, Julien N.P. Martel, Alexander W. Bergman, David B. Lindell, and Gordon Wetzstein. Implicit neural representations with periodic activation functions. In *The Thirty-fourth Annual Conference on Neural Information Processing Systems (NeurIPS)*, 2020. 2
- [25] Yannick Strümpfer, Janis Postels, Ren Yang, Luc Van Gool, and Federico Tombari. Implicit neural representations for image compression. In *European Conference on Computer Vision (ECCV)*, 2022. 2
- [26] Kun Su, Mingfei Chen, and Eli Shlizerman. INRAS: Implicit neural representation for audio scenes. In *The Thirty-sixth Annual Conference on Neural Information Processing Systems (NeurIPS)*, 2022. 2

- [27] Yang-Tian Sun, Yi-Hua Huang, Lin Ma, Xiaoyang Lyu, Yan-Pei Cao, and Xiaojuan Qi. Splatter a video: Video gaussian representation for versatile processing. In *The Thirty-eighth Annual Conference on Neural Information Processing Systems (NeurIPS)*, 2024. [1](#), [2](#), [3](#), [4](#), [5](#), [6](#), [8](#)
- [28] Penghao Wang, Zhirui Zhang, Liao Wang, Kaixin Yao, Siyuan Xie, Jingyi Yu, Minye Wu, and Lan Xu. V3: Viewing volumetric videos on mobiles via streamable 2D dynamic Gaussians. *ArXiv*, abs/2409.13648, 2024. [2](#)
- [29] Qianqian Wang, Yen-Yu Chang, Ruojin Cai, Zhengqi Li, Bharath Hariharan, Aleksander Holynski, and Noah Snavely. Tracking everything everywhere all at once. *2023 IEEE/CVF International Conference on Computer Vision (ICCV)*, pages 19738–19749, 2023. [6](#)
- [30] Shuzhe Wang, Vincent Leroy, Yohann Cabon, Boris Chidlovskii, and Jérôme Revaud. Dust3r: Geometric 3d vision made easy. *2024 IEEE/CVF Conference on Computer Vision and Pattern Recognition (CVPR)*, pages 20697–20709, 2023. [3](#)
- [31] Zhou Wang, Alan C Bovik, Hamid R Sheikh, and Eero P Simoncelli. Image quality assessment: from error visibility to structural similarity. *IEEE Trans. Image Process.*, 13(4): 600–612, 2004. [5](#)
- [32] Guanjun Wu, Taoran Yi, Jiemin Fang, Lingxi Xie, Xiaopeng Zhang, Wei Wei, Wenyu Liu, Qi Tian, and Xinggang Wang. 4D Gaussian splatting for real-time dynamic scene rendering. In *2024 IEEE/CVF Conference on Computer Vision and Pattern Recognition (CVPR)*, pages 20310–20320, 2023. [2](#), [6](#)
- [33] Xingyu Xie, Pan Zhou, Huan Li, Zhouchen Lin, and Shuicheng Yan. Adan: Adaptive Nesterov momentum algorithm for faster optimizing deep models. *IEEE Transactions on Pattern Analysis and Machine Intelligence*, 46: 9508–9520, 2022. [5](#)
- [34] Hao Yan, Zhihui Ke, Xiaobo Zhou, Tie Qiu, Xidong Shi, and Dadong Jiang. DS-NeRV: Implicit neural video representation with decomposed static and dynamic codes. In *2024 IEEE Conference on Computer Vision and Pattern Recognition (CVPR)*, pages 23019–23019, 2024. [2](#)
- [35] Vickie Ye, Zhengqi Li, Richard Tucker, Angjoo Kanazawa, and Noah Snavely. Deformable sprites for unsupervised video decomposition. *2022 IEEE/CVF Conference on Computer Vision and Pattern Recognition (CVPR)*, pages 2647–2656, 2022. [6](#)
- [36] Richard Zhang, Phillip Isola, Alexei A Efros, Eli Shechtman, and Oliver Wang. The unreasonable effectiveness of deep features as a perceptual metric. In *CVPR*, 2018. [5](#)
- [37] Xinjie Zhang, Xingtong Ge, Tongda Xu, Dailan He, Yan Wang, Hongwei Qin, Guo Lu, Jing Geng, and Jun Zhang. GaussianImage: 1000 FPS image representation and compression by 2D Gaussian splatting. In *European Conference on Computer Vision*, 2024. [2](#), [5](#), [6](#)
- [38] Ruijie Zhu, Yanzhe Liang, Hanzhi Chang, Jiacheng Deng, Jiahao Lu, Wenfei Yang, Tianzhu Zhang, and Yongdong Zhang. MotionGS: Exploring explicit motion guidance for deformable 3D Gaussian splatting. In *The Thirty-eighth Annual Conference on Neural Information Processing Systems (NeurIPS)*, 2024. [2](#)